

Subsurface Lithology Modelling of Landslide-Prone Areas in Sriharjo, Bantul Using the Geoelectrical Method

Uli Ulfa^{1*}, Hilma Lutfiana¹, Rahmawati Fitrianingtyas¹, Eko Wibowo¹, Rial Dwi Martasari¹,
Tiara Sarastika¹, Najwa Anaya², Khafidh Nur Aziz²

¹Universitas Pembangunan Nasional Veteran Yogyakarta, Indonesia

²Yogyakarta State University, Indonesia

Received : September 15, 2025	Revised : September 16, 2025	Accepted : September 19, 2025	Online : October 14, 2025
-------------------------------	------------------------------	-------------------------------	---------------------------

Abstract

Lithology modeling in a landslide-prone area using the geoelectrical method with the Wenner configuration. The research aims to determine resistivity values, subsurface lithology, and slip surfaces in Sriharjo Village, Bantul Regency, which frequently experiences landslides. This area is identified as one of the most vulnerable zones due to its steep slopes and geological conditions. Sriharjo Village, located along the Opak Fault, is a critical area where landslides have repeatedly caused significant losses. Data were collected along four 225-meter survey lines with 15-meter electrode spacing and an expansion factor up to $n = 5$. The data were processed with Res2Dinv to obtain resistivity values and two-dimensional subsurface profiles. Results show resistivity values ranging from 0.0397 Ωm to 1046 Ωm . The subsurface is divided into aquifer, clay, and breccia layers, with slip surfaces occurring in the clay and breccia layers, which display both curved and flat geometries. By identifying the slip surface and the thickness of the weathered layer above it, the landslide potential in this area can be assessed, helping to reduce casualties and minimize material losses.

Keywords *Landslide, Slip Surface, Geoelectrical, Wenner*

INTRODUCTION

Indonesia is one of the countries most vulnerable to natural disasters because of its location at the meeting point of three active tectonic plates: the Indo-Australian Plate, the Eurasian Plate, and the Pacific Plate (Syafitri et al., 2019). Tectonic activity has created mountainous terrain throughout the archipelago, with slopes ranging from gentle to very steep, which increases the risk of landslides (Hermon, 2015). Additionally, Indonesia's tropical climate, marked by heavy rainfall, acts as a key trigger for slope failures (Pabalik et al., 2015).

The Special Region of Yogyakarta (DIY) is one of the provinces most severely impacted by landslides. According to BPBD (2021), from 2015 to 2024, landslides in this area damaged 185 houses, displaced over 10,600 people, injured 30 individuals, and caused 30 deaths. Recent reports by BPBD DIY (2025) also highlight that during periods of heavy rainfall, landslides were the most common natural disaster in DIY, where Bantul Regency recorded the highest number of incidents, followed by Kulon Progo, Gunungkidul, and Yogyakarta City. In Bantul, especially in the Imogiri Subdistrict and Sriharjo Village, the area is known to be highly prone to landslides because of its steep slopes and closeness to the active Opak Fault, where seismic activity makes the hazard worse (Aminatun, 2017).

Copyright Holder:

© Uli, Hilma, Rahmawati, Eko, Rial, Tiara, Najwa, & Khafidh. (2025)
Corresponding author's email: uliulfa@upnyk.ac.id

This Article is Licensed Under:



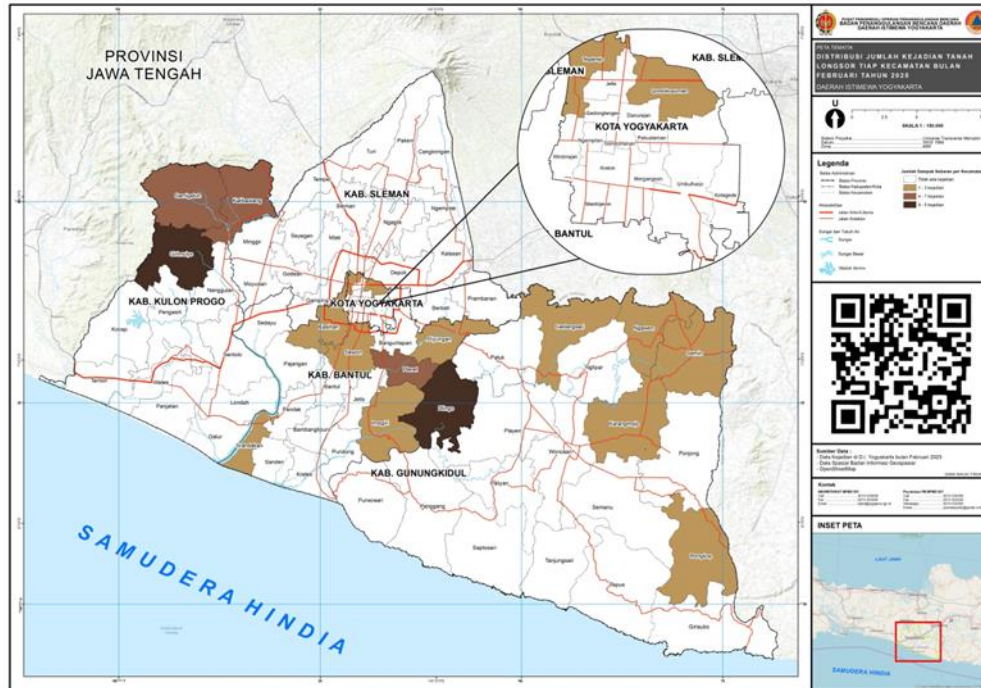


Figure 1. Landslide Hazard Map of the Special Region of Yogyakarta Province
Source: [BPBD DIY \(2025\)](#)

Previous studies have mapped landslide susceptibility in this region, emphasizing rainfall and slope gradient as the main factors ([Febriani & Jumadi, 2020](#); [Aminatun & Anggraheni, 2018](#)). However, these studies mainly focus on surface parameters. The primary knowledge gap is the limited understanding of subsurface conditions, particularly the presence and shape of slip surfaces, which fundamentally influence landslide initiation. In this regard, geoelectrical resistivity surveys offer a significant advantage, as they enable the investigation of subsurface lithology and detailed delineation of potential slip surfaces ([Purnama et al., 2016](#); [Mulyasari et al., 2020](#)). Combining resistivity data with geological observations allows for a more comprehensive understanding of slope instability mechanisms. Therefore, applying geoelectrical methods in landslide-prone areas, such as Sriharjo Village, is vital for filling knowledge gaps and improving disaster risk reduction strategies in tropical regions with high rainfall. This research was conducted with the following objectives: (1) to determine resistivity values and identify the subsurface lithology in landslide-prone areas in Sriharjo Village, Bantul Regency; (2) to determine the types of layers and the geometry of slip surfaces in these areas.

LITERATURE REVIEW

Geology of the Study Area

Based on the geological map shown in Figure 2, in the Sriharjo–Imogiri sector, the Semilir Formation (Early Miocene) consists of pumice-rich tuff and other pyroclastic deposits, representing distal silicic volcanism ([Wijayanti, 2022](#)). This unit is conformably overlain by the Nglanggaran Formation, mainly composed of andesitic volcanic breccias, lava, and volcanoclastic sandstones, indicating more proximal volcanic activity ([Warmada, 2023](#)). Recent research has revised the age of the Nglanggaran Formation to the Early–Middle Miocene (N4–N5), replacing the previous Late Oligocene interpretation based on Potassium–Argon dating ([Soeria-Atmadja et al., 1994](#); [Mulyaningsih, 2024](#)). Therefore, the stratigraphy in Sriharjo is best described as the Early Miocene Semilir Formation overlain by the Early to Middle Miocene Nglanggaran Formation.

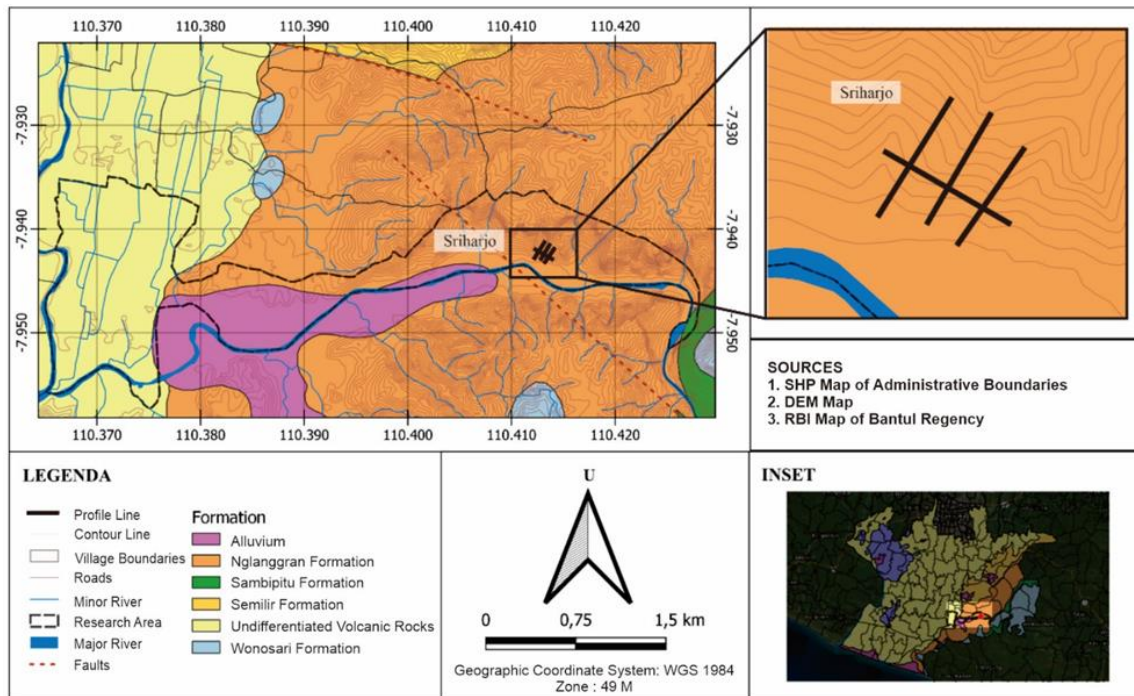


Figure 2. Geological Map of the Study Area

Source: [Rahardjo et al. \(2012\)](#)

Resistivity Method

The resistivity method is a geophysical technique used to investigate subsurface conditions by measuring the flow of electrical current through the Earth's materials. In this approach, an electric current is injected into the subsurface using a pair of current electrodes, while a separate pair of potential electrodes records the resulting potential difference. These current and voltage measurements are then used to calculate the apparent resistivity, which reveals variations in lithology, groundwater content, and structural features ([Loke et al., 2021](#)). Recent studies have highlighted the effectiveness of this method in landslide risk assessment and hydrogeological research, particularly in identifying slip surfaces and aquifer zones ([Mele et al., 2021](#); [Maiti et al., 2022](#)). The following relation mathematically expresses the apparent resistivity:

$$\rho_a = K \frac{\Delta V}{I} \quad (1)$$

where ρ_a denotes the apparent resistivity (Ωm), ΔV represents the potential difference (Volt), I represents the electrical current (Ampere), and K is the geometric factor.

The apparent resistivity values represent the types of rocks, thereby assisting researchers in interpreting subsurface conditions ([Loke et al., 2021](#)). To support this interpretation, representative resistivity values of various subsurface rock types are summarized in Table 1.

Table 1. Resistivity Values of Rocks

Lithology	Resistivity Ωm
Igneous Rock (massive)	$100 - 1.3 \times 10^7$
Clay/Clayey Soil	1-10
Wet Clay	$0,1 - 10^1$
Sandstone	$10 - 10^2$
Gravel/Breccia	$30 - 10^4$
Tuff (wet)	$10 - 10^2$

Source: [Loke et al. \(2021\)](#)

The geometric factor presented in Equation 1 is inherently connected to the electrode arrangement, particularly the spacing between current and potential electrodes. The Wenner configuration is one of the most frequently applied arrays in two-dimensional surveys due to its ability to provide high vertical resolution and maintain enough sensitivity to variations in lateral resistivity distributions ([Dahlin & Zhou, 2021](#)). This array setup includes two current electrodes (C1 and C2) and two potential electrodes (P1 and P2), arranged in a straight line with equal spacing (a). Its symmetrical design makes it easy to deploy and has proven efficacy in environmental studies, such as evaluations of landslide susceptibility and subsurface heterogeneity ([Lutfiana et al., 2025](#)). The schematic diagram of this electrode layout is shown in Figure 3.

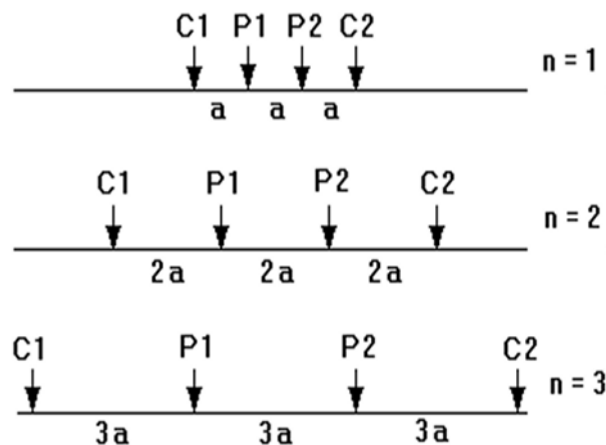


Figure 3. Electrode Arrangement of the Wenner Configuration

Source: [Loke \(2021\)](#)

based on the electrode arrangement, the geometric factor (K) for the Wenner configuration can be expressed as follows ([Reynolds, 2011](#)),

$$K = 2\pi a \quad (2)$$

RESEARCH METHOD

This research was carried out in several steps, including:

1. Literature Review, where a comprehensive review was conducted to gather background information related to landslides, geophysical methods, and the geological setting of the research area.
2. Survey, where a preliminary assessment was performed to observe field conditions, identify accessible measurement sites, and determine the suitable geoelectrical survey design.
3. Data Collection, where field data were gathered using the geoelectrical resistivity method with the Wenner configuration, which is commonly used in subsurface investigations for slope stability and landslide studies (Loke et al., 2021). Four profiles were created: three vertical and one horizontal, each 225 meters long. The electrode spacing was 15 meters, with current–potential electrode expansion up to $n = 5$. Data acquisition used a resistivity meter. Electrodes were arranged in the sequence C1–P1–P2–C2, with current injected through the current electrodes (C1 and C2), and the potential difference measured by the potential electrodes (P1 and P2).
4. Data Processing, where data were processed using three software programs: Microsoft Excel to analyze raw field measurements (current and potential) and calculate midpoints (xmid), resistance (R), geometric factor (K), and apparent resistivity values (ρ_a); Res2Dinv to invert the apparent resistivity data into two-dimensional subsurface models for each profile (Loke et al., 2021); and RockWorks to correlate the profiles and visualize the three-dimensional distribution of resistivity values. The profile map of the study area is shown in Figure 4.
5. Data Validation, in which geoelectrical data were validated through two methods: internal consistency checks, by repeating measurements at different times to ensure data stability and reproducibility; and geological correlation, by comparing the resistivity model with existing geological and geomorphological data of the study area. This comparison aimed to confirm that the interpreted subsurface lithology and slip surface geometry were consistent with field observations and regional geological maps (Hermans et al., 2012). The research profile map is shown in Figure 4.

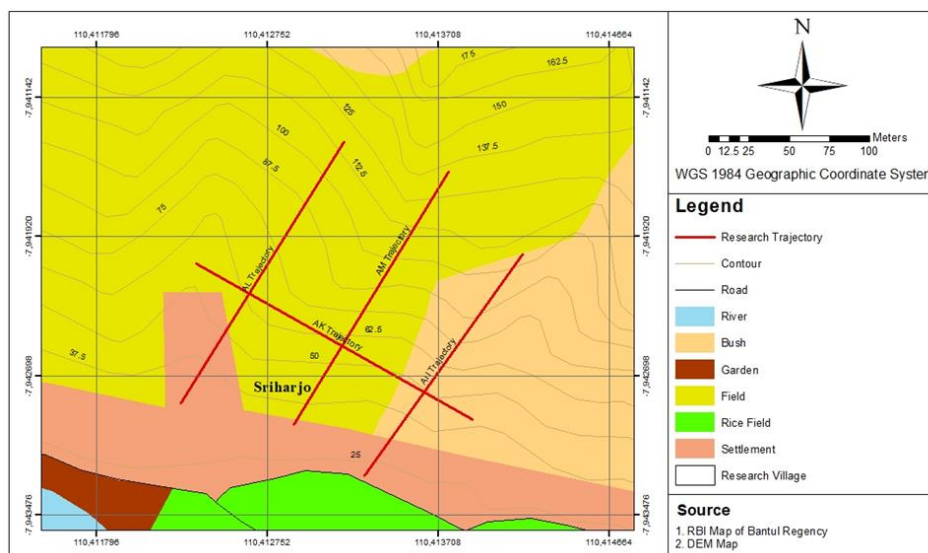


Figure 4. The Research Profile Map

FINDINGS AND DISCUSSION

Data collection was conducted in Sompok Hamlet, Sriharjo Village, Imogiri District, Bantul

Regency, bounded by the following coordinates: 7.941580° S – 7.942946° S and 110.412593° E – 110.413825° E. The geoelectrical surveys produced two-dimensional subsurface lithology models, which were further validated through three-dimensional correlation. This study makes a new contribution by demonstrating that combining geoelectrical resistivity profiling with geological field validation enables a more precise determination of slip surface shape and depth, which is essential for improved landslide hazard assessment. Field calibration identified typical resistivity values of rocks. Measurements taken from multiple surface rock outcrops served as reference points for interpretation and validation. Resistivity values below 5 $\Omega\cdot\text{m}$ identified aquifers, while claystone showed resistivity from 5 to 25 $\Omega\cdot\text{m}$. Resistivity readings above 25 $\Omega\cdot\text{m}$ were interpreted as breccia. These cutoff values align with previous research on rock resistivity ranges in near-surface environments (Loke et al., 2021).

Two-Dimension Modeling

The processed data for Profile 1 (RMS error of 14.9%) is shown in Figure 5. Based on Figure 5, Profile 1 reaches a depth of 39.2 meters with resistivity values ranging from 0.0397 – 1046 $\Omega\cdot\text{m}$. The interpretation of the profile suggests that the subsurface layers, based on resistivity values and geological conditions in the field, consist of three layers: a saturated zone, clay, and breccia. The resistivity range of 0.0397 – 0.727 $\Omega\cdot\text{m}$ is interpreted as the saturated zone, illustrated in blue. The resistivity range of 0.727 – 13.3 $\Omega\cdot\text{m}$ is likely to correspond to a clay layer, depicted in green. Meanwhile, the resistivity range of 13.3 $\Omega\cdot\text{m}$ – 1046 $\Omega\cdot\text{m}$ is interpreted as a breccia layer, illustrated in yellow. In Profile 1, a slip surface is suspected to exist between 30 meters and 82.5 meters from the starting point, at a depth of 0 meters to 12 meters below the ground surface, within the clay layer. Meanwhile, the slip surface, located between 82.5 meters and 195 meters from the starting point, is situated at depths ranging from 0 meters to 35 meters below the ground surface.

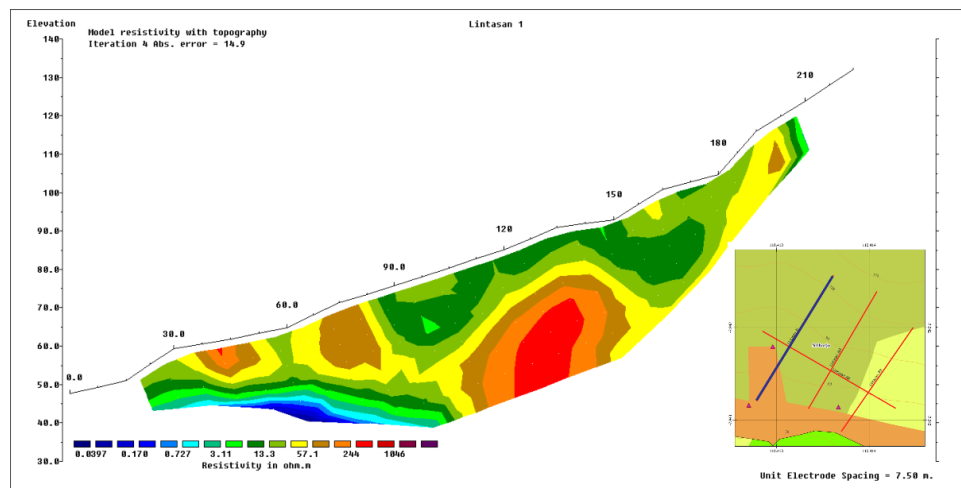


Figure 5. The Two-Dimensional Results of The Subsurface Layer for Profile 1

The processed data for Profile 2 (RMS error of 9.9%) is shown in Figure 6. Based on Figure 6, Profile 2 reaches a depth of 39.2 meters with resistivity values ranging from 0.0397 – 1046 $\Omega\cdot\text{m}$. Based on resistivity values and field geological conditions, the subsurface layers are interpreted to consist of three layers: a saturated zone, clay, and breccia. The resistivity range of 0.0397 – 0.727 $\Omega\cdot\text{m}$ is interpreted as the saturated zone, illustrated in blue, while the resistivity range of 0.727 $\Omega\cdot\text{m}$ – 13.3 $\Omega\cdot\text{m}$ is interpreted as a clay layer, illustrated in green. This layer exhibits a higher resistivity than the previous one, indicating it contains less water. Meanwhile, the resistivity range of 13.3 – 1046 $\Omega\cdot\text{m}$ is interpreted as a breccia layer, illustrated in yellow. In Profile 2, a slip surface is

suspected to be located between 135 meters and 165 meters from the starting point, at depths ranging from 0 meters to 39.2 meters below the ground surface. The clay material is interpreted as the slip surface in this profile.

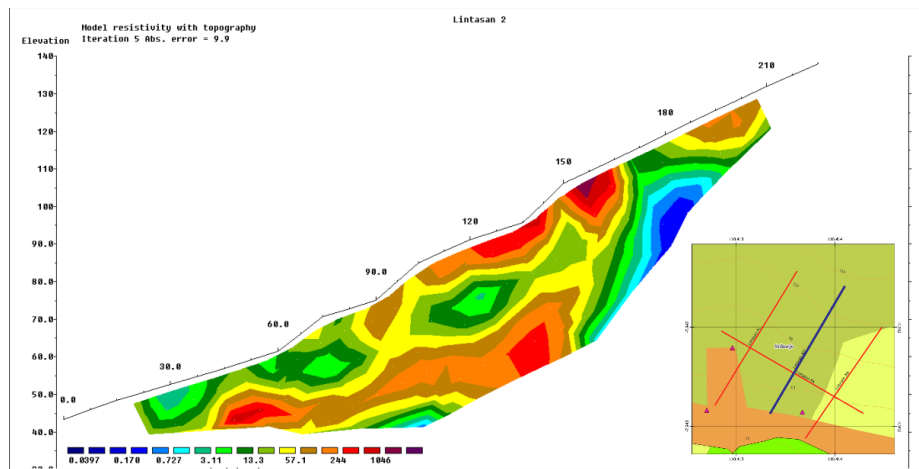


Figure 6. The Two-Dimensional Results of The Subsurface Layer for Profile 2

The processed data for Profile 3 (RMS error of 22.4%) is shown in Figure 7. Based on Figure 7, it can be observed that Profile 3 reaches a depth of 39.2 meters with resistivity values ranging from 0.558 – 352 Ωm . Based on resistivity values and field geological conditions, the subsurface layers in Profile 3 are interpreted to consist of three layers: a saturated zone, clay, and breccia. The resistivity range of 0.558 – 3.52 Ωm is interpreted as the saturated zone, illustrated in blue. The resistivity range of 3.52 Ωm – 22.2 Ωm is interpreted as a clay layer, illustrated in green. Meanwhile, the resistivity range of 22.2 Ωm – 352 Ωm is interpreted as a breccia layer, illustrated in yellow. In Profile 3, a slip surface is suspected to be located between 90 meters and 180 meters from the starting point, at a depth of 20 meters to 39.2 meters below the ground surface. The clay material is interpreted as the slip surface in this profile.

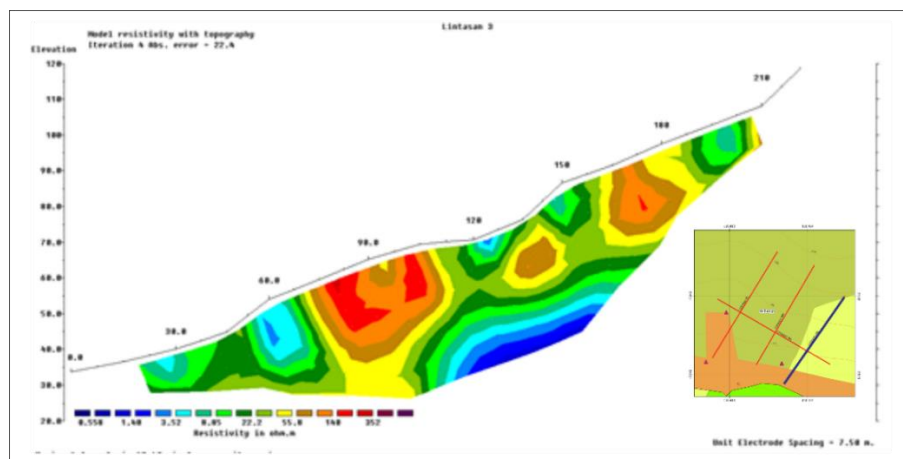


Figure 7. The Two-Dimensional Results of The Subsurface Layer for Profile 3

The processed data for Profile 4 (RMS error of 14.5%) is shown in Figure 8. Based on Figure 8, it can be observed that Profile 4 has resistivity values ranging from 0.0397 – 1046 Ωm . Based on resistivity values and field geological conditions, the subsurface layers in Profile 4 are interpreted to consist of three layers: an saturated zone, clay, and breccia. The resistivity range of 0.0397 –

0.727 Ωm is interpreted as the saturated zone, illustrated in blue, while the resistivity range of 0.727 – 13.3 Ωm is interpreted as a clay layer, illustrated in green. Meanwhile, the resistivity range of 13.3 Ωm – 1046 Ωm is interpreted as a breccia layer, illustrated in yellow.

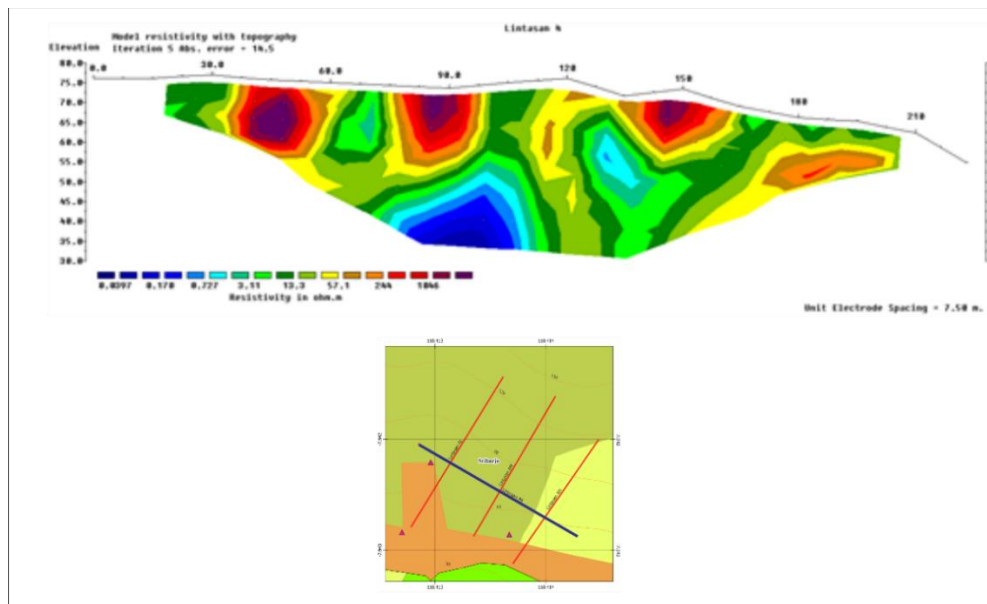


Figure 8. The Two-Dimensional Results of The Subsurface Layer for Profile 4

Three-Dimension Modeling

This three-dimensional modeling was performed to examine the correlation between measurement profiles so that the resistivity and subsurface layer types of each profile could be confirmed. The resulting correlation, which forms the three-dimensional model of the measurement profiles, is shown in Figure 9.

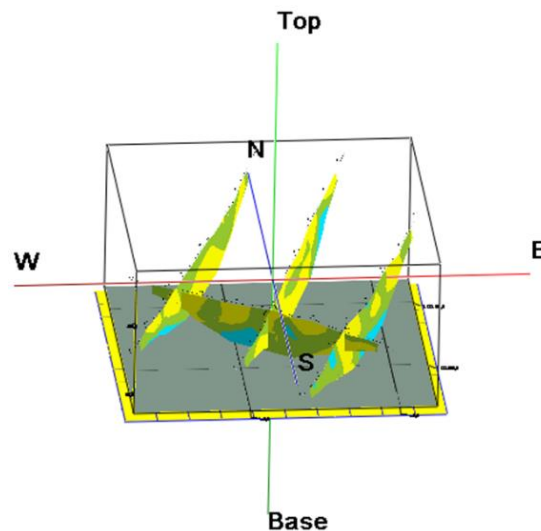


Figure 9. 3D Modelling of the Subsurface Lithology of the Measurement Profiles

Based on the two-dimensional subsurface section model and confirmed by its three-dimensional model (Figure 9), all four measurement profiles consist of the same subsurface layers, namely the aquifer, clay, and breccia layers. The layer with low resistivity is suspected to be the aquifer, the layer with medium resistivity is suspected to be clay, and the layer with high resistivity

is suspected to be breccia. Since all profiles share the same layer types, it can be concluded that the subsurface structure across the four measurement profiles is confirmed to be accurate.

The slip surface can be identified by the contact between layers with low and high resistivity, the occurrence of landslides, and rock weathering along the profile. Similar approaches have been successfully applied to delineate slip surfaces in landslide-prone zones using geoelectrical arrays (Legowo et al., 2022). Therefore, in this study, the slip surface is believed to be composed of the clay and breccia layers. When this slip surface is exposed to water, it reduces the binding force between the weathered layer above it and the slip surface itself. As a result, with a slippery surface and reduced resistance, the weathered layer above the slip surface becomes more prone to movement down the slope. The slip surface formed in profiles 1 and 2 has a curved shape, which indicates that the type of landslide that may occur is a rotational slide. Meanwhile, the slip surface in profile 3 is more level, suggesting that the landslide type that could occur is a translational slide.

CONCLUSIONS

The resistivity values in the landslide-prone area of Sriharjo Village range from 0.0397 $\Omega\cdot\text{m}$ to 1046 $\Omega\cdot\text{m}$. Analysis of four resistivity profiles reveals three main subsurface units: a saturated zone (unconsolidated layer/weathered breccia), clay, and breccia, with the slip surface typically located at the clay–breccia interface. Three-dimensional correlation confirms that these features are laterally continuous throughout the study area. The resistivity models further indicate a high potential for landslides, as thick zones of water-saturated breccia sit above a low-resistivity clay layer that acts as the slip surface. The clay layer limits vertical infiltration into the deep aquifer, increasing pore-water pressure within the overlying breccia and reducing slope stability. These findings underscore the significance of geoelectrical resistivity surveys in characterizing underground conditions associated with slope failure, providing a solid foundation for local disaster risk reduction and early warning systems.

LIMITATIONS & FURTHER RESEARCH

This study offers critical insights into the subsurface lithology and slip surfaces in Sriharjo Village. However, it has several limitations. The analysis was based exclusively on two-dimensional resistivity data, which were correlated into a three-dimensional model without borehole validation. This may potentially compromise the accuracy of lithological interpretation. Future studies should integrate additional geophysical methods, such as seismic refraction or GPR, coupled with borehole sampling and time-lapse resistivity monitoring, to improve subsurface characterization and support more reliable landslide early warning and mitigation strategies.

REFERENCES

- Aminatun, S. (2017). Kajian Analisis Risiko Bencana Tanah Longsor Sebagai Dasar Dalam Pembangunan Infrastruktur Di Desa Sriharjo Kecamatan Imogiri Kabupaten Bantul. *Teknisia*, 22(2), 372–382.
- Aminatun, S., & Anggraheni, D. (2018). Pengaruh Badai Tropis Cempaka Terhadap Kejadian Tanah Longsor di Kabupaten Bantul Yogyakarta. *Jurnal Teknologi Rekayasa*, 3(1), 105. <https://doi.org/10.31544/jtera.v3.i1.2018.105-114>.
- BPBD. (2021). *Kajian Indeks Risiko Bencana Indonesia di DIY*. https://bpbd.jogjaprovo.go.id/assets/uploads/Lap_Akhir_IRBI_DIY_21_compressed.pdf.
- BPBD DIY. (2025). *Curah hujan tinggi, tanah longsor mendominasi (March 2025 Bulletin)*. https://bpbd.jogjaprovo.go.id/detail_information/307
- Dahlin, T., & Zhou, B. (2021). A numerical comparison of 2D resistivity imaging with 10 electrode

- arrays. *Geophysical Prospecting*, 52(5), 379–398.
- Febriani, F. N. I., & Jumadi, S. S. (2020). *Analisis Kerentanan Sosial dan Ekonomi Bencana Longsorlahan di Kecamatan Imogiri Kabupaten Bantul*. Universitas Muhammadiyah Surakarta.
- Hermans, T., Nguyen, F., Robert, T., & Revil, A. (2012). Geophysical methods for hydrogeological characterization. *Near Surface Geophysics*, 10(6), 517–530
- Hermon, D. (2015). *Geografi bencana alam*. PT. Raja Grafindo Persada-Rajawali Pers.
- Legowo, B., Koesuma, S., Primastawan, A. A., & Yahya, I. (2022). Analysis of slip surface by using geoelectrical array at Wonoreja Karanganyar Regency as mitigation of landslide disaster. *IOP Conference Series: Earth and Environmental Science*, 986(1), 12030.
- Loke, M. H., Chambers, J. E., & Wilkinson, P. B. (2021). Recent developments in the inversion and interpretation of resistivity imaging data. *Near Surface Geophysics*, 19(4), 383–402.
- Lutfiana, H., Giamboro, W. S., Hidayat, W., & Sukmawan, D. I. (2025). Landslide Characteristics From Conceptual Modelling Of Weathered Layers Using Subsurface Resistivity In Sangon, Diy. *JGE (Jurnal Geofisika Eksplorasi)*, 11(2), 95–108.
- Maiti, S., Bhattacharya, B. B., & Singh, R. (2022). Application of Geoelectrical Resistivity in Landslide Hazard Zonation. *Journal of Applied Geophysics*, 198, 104577.
- Mele, M., Perrone, A., & Piscitelli, S. (2021). Electrical resistivity tomography for investigating landslide-prone slopes: Recent advances and perspectives. *Engineering Geology*, 293, 106299.
- Mulyaningsih, S., Putong, R., Prima, A., Hidayah, R. A., & Kiswiranti, D. (2024). Volcanic Evolution of the Southern Mountain Neogene Magmatic Belt in Baturagung Range Central Java, Indonesia. *Journal of Geoscience, Engineering, Environment, and Technology*, 9(04), 400–419. <https://doi.org/10.25299/jgeet.2024.9.04.18461>.
- Mulyasari, R., Darmawan, I. G. B., Effendi, D. S., Saputro, S. P., Hesti, H., Hidayatika, A., & Haerudin, N. (2020). Aplikasi Metode Geolistrik Resistivitas Untuk Analisis Bidang Gelincir Dan Studi Karakteristik Longsor Di Jalan Raya Suban Bandar Lampung. *JGE (Jurnal Geofisika Eksplorasi)*, 6(1 SE-Articles), 66–76. <https://doi.org/10.23960/jge.v6i1.61>.
- Pabalik, I., Ihsan, N., & Arsyad, M. (2015). Analisis Fenomena Perubahan Iklim dan Karakteristik Curah Hujan Ekstrim di Kota Makassar. *Jurnal Sains Dan Pendidikan Fisika (JSPF)*, 11(1), 88–92.
- Purnama, A. Y., Darmawan, D., & Wibowo, N. B. (2016). Interpretasi Bawah Permukaan Zona Kerentanan Longsor di Desa Gerbosari Kecamatan Samigaluh Kabupaten Kulonprogo Menggunakan Metode Geolistrik Konfigurasi Dipole-Dipole. *Jurnal Pendidikan Matematika dan Sains UNY*.
- Rahardjo, W., Sukandarrumidi, & Rosidi, H. M. (2012). *Peta Geologi Lembar Yogyakarta, Jawa skala 1:100.000*. Pusat Survei Geologi, Badan Geologi.
- Reynolds, J. M. (2011). *An introduction to applied and environmental geophysics*. John Wiley & Sons.
- Soeria-Atmadja, R., Maury, R. C., Bellon, H., Pringgoprawiro, H., Polve, M., & Priadi, B. (1994). Tertiary magmatic belts in Java. *Journal of Southeast Asian Earth Sciences*, 9(1–2), 13–27.
- Syafitri, Y., Bahtiar, B., & Didik, L. A. (2019). Analisis pergeseran lempeng bumi yang meningkatkan potensi terjadinya gempa bumi di Pulau Lombok. *Konstan-Jurnal Fisika Dan Pendidikan Fisika*, 4(2), 139–146.
- Warmada, I. (2023). *Southern Mountains Stratigraphy and Volcanic Arc Evolution*. UGM Geological Review Series.
- Wijayanti, H. D. K. (2022). Stratigraphy of the Semilir and Nglangeran Formations along the Pilangrejo–Nglipar traverse, Gunungkidul, Yogyakarta. *Jurnal Geosainstek*, 8(2), 69–79.